



RESEARCH

# Flow patterns of (3 + 1)-dimensional solutions of the Charney-Obukhov equation

N. N. Myagkov · A. G. Kudryavtsev

Received: 12 March 2024 / Accepted: 26 April 2024 / Published online: 17 May 2024  
© The Author(s), under exclusive licence to Springer Nature B.V. 2024

**Abstract** We consider flow patterns for exact solutions of the (3 + 1)-dimensional nonlinear nondissipative quasi-geostrophic potential vorticity equation, also known as the Charney–Obukhov equation, for Rossby vortices in the ocean propagating along the zonal direction with a constant velocity  $V$ . The following results are obtained: (a) For a given value of  $V$  the vortices are localized in the vicinity of one or several planes  $z = z_{ci}$ ,  $i = 1, 2, \dots, L$ , where  $0 \leq z_{ci} \leq H$  and  $L$  is the number of such planes, which are determined by the zonal flow included in the exact solution of the Charney–Obukhov equation; (b) Heton-like model of a baroclinic dipole, whose vortices are localized in two horizontal  $XY$ -planes, located one above the other. The heton can propagate both to the west and to the east with a velocity significantly exceeding the Rossby wave speed, this heton model is realized both in cylindrically symmetric solutions and in spherically symmetric solutions; (c) We consider a non-central “collision” of vortex monopoles and dipoles localized in the horizontal  $XY$ -plane, depending on their polarization and orientation in space. The “collision” of vortices is described as a sequence of stationary states, each of which is an exact solution to the Charney–Obukhov equation. The result of a non-central “collision”: two unipolar vortices merge, two

oppositely polarized vortices form a dipole, two oppositely directed dipoles form a tripole upon “collision”.

**Keywords** Charney—Obukhov equation · Ocean · Flow patterns · Hetons · Collision of vortices, · Collision of dipolar vortices

## 1 Introduction

It is well known that a large number of mesoscale circulations of the Earth’s atmosphere and ocean are described by the nonlinear non-dissipative quasi-geostrophic potential vorticity equation [1, 2], also known as the Charney–Obukhov equation. Let us immediately note that equations of the Charney–Obukhov type are found not only in problems of geophysics, but also in problems of plasma physics (where it is known as the Charney–Hasegawa–Mima equation) [2, 3], mechanics of biological fluids [4] and, finally, in problems of astrophysics in connection with the description of the dynamics of astrophysical disks (e.g., [5]).

Until recently, it was believed (see, for example, [2]) that the Charney—Obukhov equation cannot be integrated by the inverse scattering transformation method [6] and therefore does not have  $N$ —soliton solutions that would make it possible to analytically study the formation and interaction of Rossby waves

N. N. Myagkov · A. G. Kudryavtsev (✉)  
Institute of Applied Mechanics, Russian Academy of Sciences, Moscow 125040, Russia  
e-mail: kudryavtsev\_a\_g@mail.ru

and vortices. The recently discovered Lax Representation of the Charney–Obukhov Equation [7] has not yet led to the appearance of publications with new analytical solutions.

Research efforts were aimed at finding exact solutions to the Charney–Obukhov equation in the form of single localized vortices in the absence of a background zonal flow. The number of found 3D solutions of this kind is very limited. These include: Berestov's solution [2] in the form of a solitary spherical dipole Rossby vortex, Kaladze's solution [8] in the form of a solitary cylindrical monopole Rossby vortex. In addition, in many works to obtain multi-wave solutions, the potential vorticity equation is reduced by the perturbation methods into one of the known integrable equations (that is the Korteweg–de Vries equation, modified Korteweg–de Vries equation, Boussinesq equation and so on) modeling Rossby waves amplitude (a more detailed review of these works can be found in articles [9–11]).

The purpose of this work is to analyze and interpret the flow structures of exact solutions of the (3 + 1)-dimensional nonlinear Charney–Obukhov equation for Rossby waves and vortices in the ocean propagating along the zonal direction at a constant velocity. These solutions were found by us in recent works [12–14].

The article is organized as follows. Section 2 considers exact solutions of the (3 + 1)-dimensional nonlinear Charney–Obukhov equation. We introduce the concept of planes of localization of vortex solutions. We show that the exact solutions found include heton-like vortices. Note that a heton is the simplest model of a baroclinic vortex capable of transferring heat in the ocean, so much attention is paid to their study (see, for example, [15–20]). Section 3 provides analysis and visualization of heton-like patterns for cylindrical and spherically symmetric solutions. Section 4 considers the collision of two vortices of the same and opposite polarity, localized in the horizontal  $XY$ -plane. The non-central collision of two vortex dipoles with the formation of a tripole is also considered. Conclusions are drawn in Sect. 5.

## 2 Exact solutions of the Charney–Obukhov equation

We have considered the (3 + 1)-dimensional nonlinear Charney–Obukhov equation in the  $\beta$ -plane approximation

$$\frac{\partial}{\partial t}(\Delta\psi) + J(\psi, \Delta\psi) + \beta \frac{\partial}{\partial x}\psi = 0 \quad (1)$$

Equation (1) is written in dimensionless variables in the standard way [1]. In Eq. (1)  $\psi$  is the dimensionless geostrophic stream function, bearing the sense of relative pressure perturbation;  $\beta$  is the dimensionless meridional (northern) gradient of Coriolis parameter;  $\Delta = \frac{\partial^2}{\partial x^2} + \frac{\partial^2}{\partial y^2} + \frac{\partial}{\partial z} \left( \frac{1}{S} \frac{\partial}{\partial z} \right)$  and  $J(a, b) = \frac{\partial a}{\partial x} \frac{\partial b}{\partial y} - \frac{\partial a}{\partial y} \frac{\partial b}{\partial x}$  is the two-dimensional Jacobian. We assume that the stratification parameter  $S$  is a constant, which can be set to  $S = 1$  without loss of generality. As usual, we assume that the  $x$ -coordinate is east, the  $y$ -coordinate is north, and the  $z$ -coordinate is up. We have taken the boundary conditions [1] with a flat bottom and a rigid lid as

$$\frac{d_0}{dt} \frac{\partial \psi}{\partial z} = 0 \text{ at } z = 0 \text{ and } z = H \quad (2)$$

where  $H$  – the ocean depth ( $0 \leq z \leq H$ ) and  $\frac{d_0}{dt} = \frac{\partial}{\partial t} + V_x \frac{\partial}{\partial x} + V_y \frac{\partial}{\partial y}$ ,  $V_x = -\frac{\partial}{\partial y}\psi$ ,  $V_y = \frac{\partial}{\partial x}\psi$ . Boundary conditions (2) mean that the vertical velocity is zero at  $z = 0$  and  $z = H$ .

All exact solutions we found [12–14] of Eq. (1) with boundary conditions (2) have the form

$$\psi(x - Vt, y, z) = C\phi(x - Vt, y, z) + \Psi(y, z) \quad (3)$$

where  $\Psi(y, z) = -U(z; V)y$ ,  $U(z; V)$ —the velocity of the steady zonal background flow which depends on the drift velocity  $V$  and other constants included in the solution, and  $C$ —arbitrary constant. Note that the second term on the right side  $\Psi(y, z)$  in (1) is itself a solution of the Charney–Obukhov equation corresponding to the case  $C = 0$ , but the first term  $C\phi(x - Vt, y, z)$  is not. As was shown in [14], the solutions found have the property of partial superposition: the first term on the right side of (3) can be a superposition of trigonometric functions and cylindrically symmetric Bessel functions in the horizontal plane, or a superposition of spherically symmetric functions along the vertical coordinate. That is, the solutions found [14] represent a partial superposition of

“elementary solutions”, having the same background flow, which we obtained earlier in [12] and [13]. From the found solutions to Eq. (1) with boundary conditions (2), we can select those that have a “separation” of variables. They have the form

$$\psi = f(z) \cdot F(x - Vt, y) - U(z; V)y \tag{4}$$

The function  $F$  in (4) satisfies the equation.

$$\frac{\partial^2}{\partial s^2} F(s, y) + \frac{\partial^2}{\partial y^2} F(s, y) + K_r^2 F(s, y) = 0 \tag{5}$$

We will consider the following particular solution to Eq. (5)

$$F(x - Vt, y) = \sum_{i=1}^{N_1} C_i \sin(k_i(x - x_i - Vt)) + \sqrt{K_r^2 - k_i^2} (y - y_i) + \sum_{j=1}^{N_2} C'_j J_0 \left( K_r \sqrt{(x - x'_j - Vt)^2 + (y - y'_j)^2} \right) \tag{6}$$

where  $J_0(\cdot)$  is the Bessel function of the first kind of order zero;  $N_1 \geq 1$  and  $N_2 \geq 1$  – arbitrary positive integers;  $K_r, k_i, C_i, C'_j, x_i, x'_j, y_i, y'_j$  – arbitrary constants,  $K_r^2 \geq k_i^2$ . The second sum on the right side of (6) is a linear superposition of cylindrically symmetric Rossby vortices, localized in one or several planes and propagating at a constant velocity  $V$  without changing the shape of the function  $\psi$ .

For a given value of the velocity parameter  $V$ , vortices and waves are localized in  $z$ —neighborhood of the plane  $z = z_c$ , which is defined [14] as a solution to the equation

$$U(z_c; V) = 0, \quad 0 \leq z_c \leq H \tag{7}$$

Equation (7) may have no solutions or have one, two or more solutions depending on  $V$  and other parameters included in  $U$ . As an example, consider the dependences  $z_c(V)$  for solution (11), obtained from the equation

$$U(z_c; V) \equiv V - \frac{\beta(\sin(Kz_c)M + \cos(Kz_c) - 1)}{K^2} = 0 \tag{8}$$

where  $K = \sqrt{K_r^2 + k_z^2}$  and parameter  $M$  (12) depends on parameters  $H, K$  and  $k_z$ . Thus, Eq. (8) gives the dependence of  $z_c$  on the velocity  $V$  for various values

of parameters  $H, \beta, K_r$  and  $k_z$ . The choice of the last two parameters makes it possible to effectively control the dependence of the location of the localization plane  $z = z_c(V)$  on the drift velocity of the vortices  $V$  in this plane.

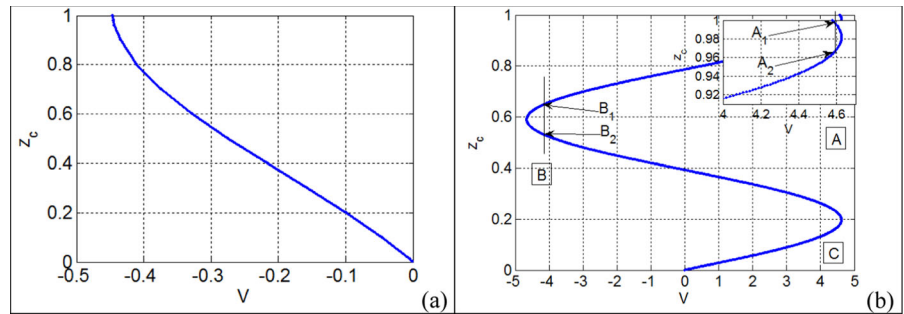
Figure 1a shows the dependence  $z_c(V)$  for the values of the parameters  $H = \beta = 1, K_r = 1.75, k_z = 1.5$ . It can be seen that for these parameter values the dependence  $z_c(V)$  has one branch with acceptable velocity values  $-0.446 \leq V \leq 0.0$ , that is, depending on the value of the velocity  $V$ , the solution to Eq. (8) can describe a vortex flow in one localization plane or not describe any vortex flow.

Figure 1b shows the dependence  $z_c(V)$  for parameter values  $H = \beta = 1, K_r = 2\pi, k_z = 1.575\pi$ . It can be seen that for these parameter values the dependence  $z_c(V)$  has three reversals and four segments, that is, depending on the value of the velocity  $V$ , the solution to Eq. (8) can describe up to 4 localization planes with a vortex flow or not describe any vortex flow. Acceptable velocity values  $V$  lie between  $V_{\min} = -4.66$  ( $z_c = 0.595$ )—reversal  $B$  and  $V_{\max} = 4.627$  ( $z_c = 0.981$  or  $0.196$ )—reversals  $A$  and  $C$ . The turning-points in Fig. 1b are critical points: when passing these points, two oppositely polarized vortices, having the same speed  $V$  and a common vertical axis of symmetry, are born (or disappear) as  $V$  changes. Supercritical solutions (11–13) in the vicinity of turning points  $A, B$  and  $C$  are baroclinic dipoles, they are discussed in Sect. 3 of the article. In accordance with the accepted terminology (see, for example, [15, 16]), we will further call such baroclinic dipoles hetons.

For the case presented in Fig. 1b, at velocities  $V_{\min} < V \leq 0$  there is a solution in the form of a heton with two vortices localized in 2 different horizontal planes  $z = z_{ci}(V), i = 1, 2$ , where  $z_{ci}(V)$  are defined as solutions to Eq. (8), for example, at points  $B_1$  and  $B_2$ . At velocities  $0 < V \leq 4.577$ , there is a solution in the form of a heton of three vortices with alternating polarity, localized in 3 different horizontal planes with a common vertical axis, the equations of the vortex localization planes are determined similarly to the previous case; at velocities  $4.577 < V < V_{\max}$ , there is a solution in the form of two hetons in the near-surface (for example, at points  $A_1$  and  $A_2$ ) and near-bottom (for example, at two corresponding points near the reversal  $C$ ) regions with a large gap between them.

As is known, in hydrodynamics, a velocity rotor, that is, relative vorticity, is used to describe a rotating

**Fig. 1** Dependence of the position of the localization plane  $z = z_c$  on the vortex drift velocity  $V$  in this plane for solution (11) at parameter values  $H = \beta = 1$  and **a**  $K_r = 1.75, k_z = 1.5$ ; **b**  $K_r = 2\pi, k_z = 1.575\pi$



fluid. By the value of the relative vorticity  $\omega$  we can judge whether the vortex is strong or weak, and by the sign of the vertical component  $\omega_z$  we determine the polarity of the vortex: a cyclone or an anticyclone. Here we will be interested only in the vertical component of vorticity  $\omega_z$ , which for the solution (4), (5) has the form

$$\begin{aligned} \omega_z &= \frac{\partial V_y}{\partial x} - \frac{\partial V_x}{\partial y} = f(z) \left( \frac{\partial^2}{\partial x^2} + \frac{\partial^2}{\partial y^2} \right) F(x - Vt, y) \\ &= -f(z) K_r^2 F(x - Vt, y) \end{aligned} \tag{9}$$

Thus, in the localization plane  $z = z_c$  for solutions of the form (4) from (9) we have

$$\omega_z = -K_r^2 \psi(x - Vt, y, z_c) \tag{10}$$

that is, the value  $\omega_z$  is determined by the geostrophic stream function taken with the opposite sign.

### 3 Heton-like models

We consider a solution of the form (4), published in [14]

$$\begin{aligned} \psi &= \sin(k_z z) F(x - Vt, y) \\ &+ \left( -V + \frac{\beta(\sin(Kz)M + \cos(Kz) - 1)}{K^2} \right) y \end{aligned} \tag{11}$$

where  $K^2 = K_r^2 + k_z^2$ ;  $K_r$  and  $k_z$ —arbitrary constants,

$$M = \frac{K \sin(k_z H) \sin(KH) + k_z \cos(k_z H) \cos(KH) - k_z \cos(k_z H)}{K \sin(k_z H) \cos(KH) - k_z \cos(k_z H) \sin(KH)} \tag{12}$$

The function  $F(x - Vt, y)$  in (11) satisfies Eq. (5) and can be taken in the following form

$$F(x - Vt, y) = \sum_{j=1}^N C_j J_0 \left( K_r \sqrt{(x - a_j - Vt)^2 + (y - b_j)^2} \right) \tag{13}$$

where  $J_0(\cdot)$  is the Bessel function of the first kind of order zero;  $C_j, a_j, b_j$ —arbitrary constants;  $N \geq 1$ —is a positive integer indicating the number of cylindrically symmetric vortices considered in the problem.

From (9) and (11) we have

$$\omega_z = -\sin(k_z z_c) K_r^2 F(x - Vt, y) \tag{14}$$

From (13) and (14) it is clear that the intensity of individual (non-interacting) vortices is determined by the values of the coefficients  $\sin(k_z z) K_r^2 C_j$ , and their polarity, for fixed  $K_r$  and  $k_z$ , is determined by the signs of the coefficients  $C_j$ . If  $\sin(k_z z) > 0$ , then a negative value of  $C_j$  will correspond to a cyclone (counterclockwise rotation), and a positive value of  $C_j$  will correspond to an anticyclone (clockwise rotation).

We model the hetons within the framework of solution (11–13) for  $N = 1$  and values  $H = \beta = 1, K_r = 2\pi, k_z = 1.575\pi$ . As is already clear from Fig. 1b, a necessary condition for constructing a heton is the presence of turning points on the dependence  $z_c(V)$ . In Fig. 1b there are three such turns, they are designated by the letters A, B and C. Let us choose for modeling three pairs of closely spaced localization planes, which are specified by points  $A_1(4.6, 0.995)$  and  $A_2(4.6, 0.968)$ ,  $B_1(-4.113, 0.65)$  and  $B_2(-4.113, 0.5276)$ ,  $C_1(4.6, 0.2096)$  and  $C_2(4.6, 0.18236)$  i.e. in each pair of vortices the upper and lower vortices have the same velocity. In addition, hetons A and C have the same velocity  $V = 4.6$ .

Streamlines of the hetons in the XZ plane (at  $y = 0$ ) are shown in Fig. 2a–c. Designations of hetons in the caption to this figure by capital letters A, B, C correspond to Fig. 1b. It can be seen that the vortices

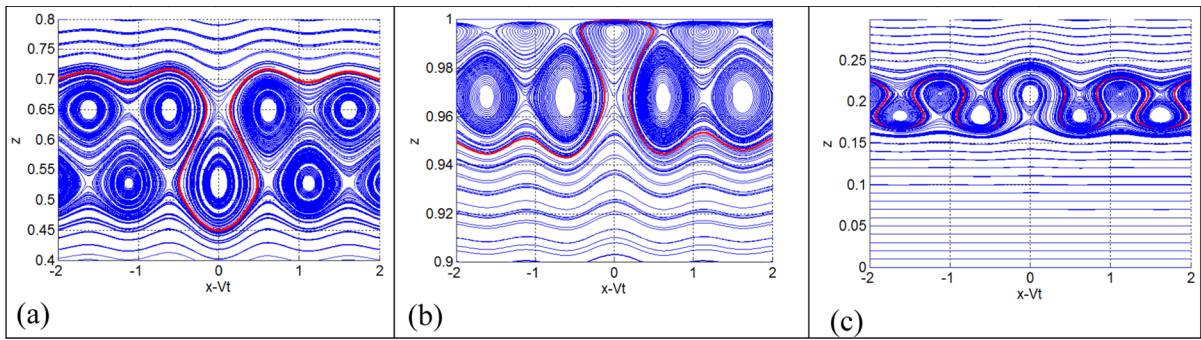


**Fig. 2** Streamlines of the hetons in the XZ plane in section  $y = 0$ . Parameter values in solution (11–13):  $H = \beta = 1, N = 1, a_1 = b_1 = 0, K_r = 2\pi, k_z = 1.575\pi$ . The parameter  $C_1$ , which

determines the amplitude, and the velocity  $V$  differ for different hetons; **a** heton  $B, V = -4.113, C_1 = 2 \cdot 10^{-3}$ ; **b** and **c**—hetons  $A$  and  $C$ , respectively, with  $C_1 = 2 \cdot 10^{-4}$  and  $V = 4.6$

in each heton have a common axis of symmetry, a common center and common streamlines—one of the common streamlines is highlighted in red. Hetons  $A$  and  $C$  have the same speed and the same axis of symmetry; they appear in solution (11)–(13) simultaneously. However, in the figures (Fig. 2b–c) they are given separately due to the fact that in the general picture their structure would be indistinguishable, since their width  $\Delta z_c$  is much less than the ocean depth  $H$ , which in Fig. 2 was taken equal to one. Figure 2a–c show that the localization planes have a finite thickness, which can be estimated as  $\Delta z_c = O((C_1/H)^{1/2})$ .<sup>1</sup>

Similarly, for the solution (11–13) for  $N = 2$ , a vertical vortex quadrupole is constructed (Fig. 3), all vortices of which propagate with the same velocity  $V = -4.113$ . In the  $XY$  plane, the coordinates of the left pair of vortices are  $(-2, 0)$ , of the right pair of vortices are  $(2, 0)$ . The cores of vortex monopoles are visible as compact thick colored spots: the red spot is an anticyclone, the blue spot is a cyclone (Fig. 3b, c).

The dimensionless meridional gradient of Coriolis parameter in (1) is  $\beta = \frac{\beta_0 L^2}{U} = O(1)$  [1], where  $L$  and  $U$  are characteristic horizontal length and velocity scales. Let  $L = L_R$ , where  $L_R$  is the baroclinic Rossby radius of deformation, which is a typical horizontal scale. Then we have the estimate  $U = \beta_0 L_R^2$ , i.e. the characteristic horizontal velocity is approximately equal to the Rossby wave speed, which is estimated at  $1\text{--}2 \text{ cm s}^{-1}$  for mid-latitudes [21]. Thus, the selected hetons in Fig. 1b can propagate both east and west

with the velocities, significantly exceeding the Rossby wave speed. It is known [21] that for the first time the above properties were discovered for horizontal pairs of vortices, called “modons.”

A baroclinic dipole—heton can be constructed not only on the basis of a cylindrically symmetric solution of type (4) with a function  $F$  of the form (13), but also on the basis of a spherically symmetric solution [13, 14]. Let us consider a spherically symmetric solution that takes into account the partial superposition of solutions with vertically shifted centers [14]

$$\psi = \sum_{i=1}^N \frac{C_i \sin(K_n R_i + a_i)}{R_i} + \left( \frac{\beta(\cos(K_n z) - 1)}{K_n^2} - V \right) y \tag{15}$$

where  $R_i = \sqrt{(x - Vt)^2 + y^2 + (z - z_i)^2}, K_n = \frac{2\pi \cdot n}{H}, N$  and  $n = 1, 2, 3, \dots, C_i, a_i, z_i$  are arbitrary constants. Equation (7) for solution (15) has the form

$$U(z_c; V) \equiv - \left( \frac{\beta(\cos(K_n z_c) - 1)}{K_n^2} - V \right) = 0 \tag{16}$$

Note that the velocity  $V$  is also a free parameter of the problem. It can be seen from the (16) that at  $n = 1$  the vortices are located in one ( $z_c = 0.5H$ ) plane or two ( $z = z_c$  and  $z = H - z_c$ ) planes where  $z_c$  is any number from the interval  $0 \leq z_c < 0.5H$ . The vortices have the same drift velocity  $V = \frac{\beta(\cos(K_1 z_c) - 1)}{K_1^2}$ . At  $n = 2$  the vortices are located in two, three or four planes  $z = z_c, z = H - z_c, z = 0.5H - z_c$  and  $z = 0.5H + z_c$  where  $z_c$  is any number from the interval  $0 \leq z_c \leq 0.25H$ , and so on.

<sup>1</sup> Recall that here the ocean depth  $H$  is a dimensionless quantity.



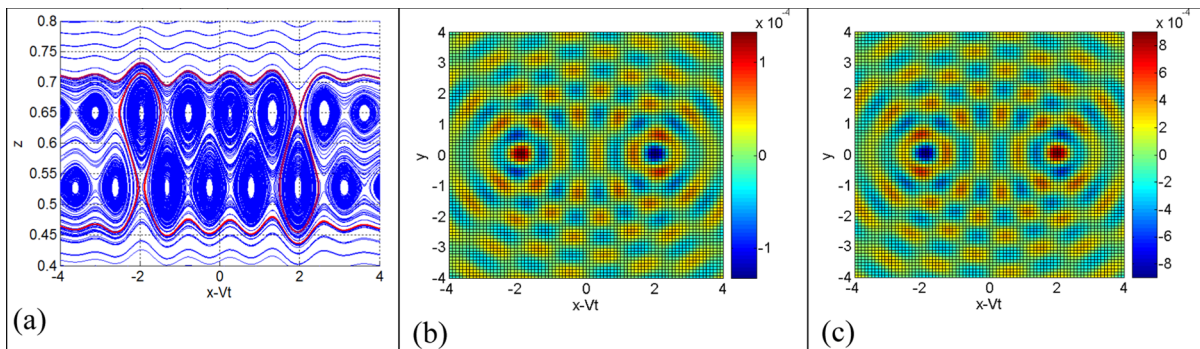


**Fig. 3** Baroclinic quadrupole. Parameter values in solution (11)—(13):  $H = \beta = 1$ ,  $N = 2$ ,  $C_1 = -C_2 = 2 \cdot 10^{-3}$ ,  $a_1 = -a_2 = 2$ ;  $b_1 = b_2 = 0$ ;  $K_r = 2\pi$ ,  $k_z = 1.575\pi$ ,  $V = -4.113$ . **a** Streamlines of the baroclinic quadrupole. View in

It is easy to see from (16) that vortices can exist only in the velocity range  $-\frac{2\beta}{K_1^2} \leq V \leq 0$ . Consider the case  $N = 1$  and  $n = 1$  when the vortices are located in one ( $z_c = 0.5H$ ) plane at  $V = -\frac{2\beta}{K_1^2}$  or two ( $z = z_c$  and  $z = H - z_c$ ) planes, where  $-\frac{2\beta}{K_1^2} < V < 0$ . The result of visualization of solution (15) in this case is shown in Fig. 4. At the turning point  $V = -\frac{2\beta}{K_1^2}$ ,  $z_c = \frac{1}{2}H$ , only one vortex is possible. Figure 4a shows the  $XZ$  view of this vortex in the section  $y = 0$ , and Fig. 4b shows the center of the vortex as an  $XY$  view in the  $z = \frac{1}{2}H$  plane. Figure 4c shows a baroclinic dipole—heton, the vortices of which are located in the planes  $z = 0.45H$  and  $z = 0.55H$  and have the same velocity  $V = -\frac{1.95\beta}{K_1^2}$ . The streamline that is common to both vortices is highlighted in red.

Let us now consider the case of superposition of two spherical solutions, i.e. when  $N = 2$  in solution (15). For a set of parameters  $n = 1$  и  $H = \beta = 1$ ,  $C_1 = 0.001$ ,  $C_2 = -0.001$ ,  $a_1 = a_2 = 0$ ,  $z_1 = 10$ ,  $z_2 = -10$  and  $V = -4.942 \cdot 10^{-2}$  we again have a pair of vortices localized in the planes  $z = 0.45$  and  $z = 0.55$ , forming a heton. Figure 5a shows the  $XZ$  view at  $y = 0$  section. It can be seen that the vortices have a common core at the center of the vortices and common streamlines passing through this core and its neighboring eddies (one of these streamlines is highlighted in red in Fig. 5a). This core is significantly larger than the size of the core in a similar solution without superposition (Fig. 4a).

For completeness, Fig. 5b, c shows geostrophic stream functions  $\psi(x,y)$  in the localization planes

$XZ$ -plane in section  $y = 0$ ; **b** and **c**  $XY$  view of the geostrophic stream function  $\psi(x,y,z)$  in localization planes  $z = 0.65$  and  $z = 0.5276$ , respectively

$z = 0.45$  and  $z = 0.55$ . It can be seen that each vortex consists of a central part (core) and flows in the form of concentric rings with alternating directions of rotation. In this case, the core and rings of the lower vortex and the upper vortex, located one above the other, have different polarities.

#### 4 Simulation of the collision of localized vortices in solution (11)

We consider solution (11) with function  $F(x - Vt, y)$  in form (13).

We will call the solution (11), (13) at  $N = 1$  a monopole, a dipole the solution at  $N = 2$ , when the centers of the monopoles are at a sufficiently close distance from each other, the same for a quadrupole at  $N = 4$  and so on. It is clear that the monopole consists of the most intense central vortex (core) and concentric vortex rings with alternating positive and negative values of the geostrophic stream function  $\psi^2$ . The monopole, depending on the sign  $\psi$  of the central vortex, will be called an anticyclone ( $\psi > 0$ ) or a cyclone ( $\psi < 0$ ). Let us immediately note the difference between the localized solution (11), (13) and the Larichev-Reznik soliton [2]: the Larichev-Reznik soliton decays exponentially at infinity, while the solution (11), (13) has the asymptotic behavior

<sup>2</sup> In the plane of localization of the vortex  $z = z_c$  the relation (7) is satisfied, therefore, the sign of  $\Psi$  in the plane of localization with distance from the center of the vortex is determined by the Bessel function  $J_0(K_r r)$ .

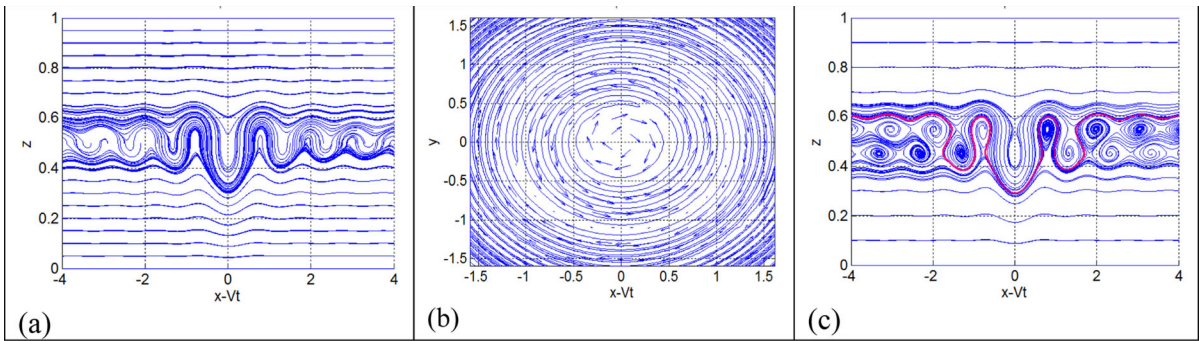


**Fig. 4** Flow patterns of solution (15) for parameter values  $N = 1, n = 1, H = \beta = 1, C_1 = 0.001, a_1 = 0, z_1 = 0$ . **a** XZ view of the vortex (section  $y = 0$ ) at the turning point  $z_c = 0.5, V = - 5.07 \cdot 10^{-2}$ ; **b** XY view of the vortex at the turning point in

the plane  $z = 0.5$ ; **c** XZ view of a heton in the section  $y = 0$ , vortices are localized in the planes  $z = 0.45$  and  $z = 0.55$ , heton velocity  $V = - 4.94 \cdot 10^{-2}$

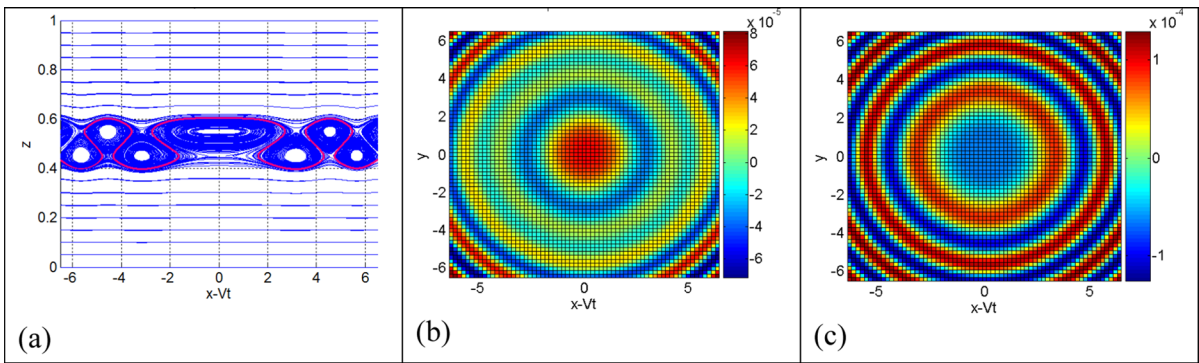


**Fig. 5** Flow patterns of solution (15) in XZ and XY planes with parameter values  $N = 2, n = 1, H = \beta = 1, C_1 = 0.001, C_2 = - 0.001, a_1 = a_2 = 0, z_1 = 10, z_2 = -10$ . **a** Streamlines in XZ-plane at  $y = 0$  at  $z_c = 0.45$  and  $0.55$ . The streamline that is

common to both vortices is shown in red. **b** Geostrophic stream function  $\psi(x,y)$  in XY-plane  $z = 0.55$ . **c** Geostrophic stream function  $\psi(x,y)$  in XY-plane  $z = 0.45$

$\psi \sim r^{-1/2}$  at  $r \rightarrow \infty$ , that is this solution is not a soliton solution in the generally accepted sense.

The “collision” of localized cylindrically symmetric Rossby vortices in the form of monopoles or dipoles is considered. The collision of something with something, generally speaking, implies evolution in time, since the collision process itself is dynamic. Solutions of the form (4) (this type of solution also includes solution (11)) describe a stationary flow against the background of a zonal flow, that is, the time parameter is not included explicitly in this solution, but only implicitly through the running coordinate  $x - Vt$ .

However, the solution includes constant parameters  $a_i, b_i$ , by changing which we can place the centers of monopoles (or dipoles) at a given distance from each other, modeling both the process of their removal from

each other and their approach. Let us assume, for example, that the shift parameters along the zonal coordinate  $a_i, i = 1, 2$ , depend on one parameter as follows:  $a_1 = a$  and  $a_2 = - a$ . Then, by changing the parameter  $a$ , we modeling both the process of monopoles moving away from each other and their approach. It must be understood that in this way we model a sequence of stationary solutions, but not the evolution of the flow in the generally accepted sense. For this reason, the term “collision” above was placed in quotation marks, which we omit below.

Throughout this section we took the parameter values  $H = 1, \beta = 1, K_r = 1.75$  and  $k_z = 1.5$ . For these parameter values, the dependence of  $z_c$  on  $V$ , obtained from (7) and (8) for solution (11), has a monotonic character (Fig. 1a), that is, each value  $0 \leq z_c \leq H$  corresponds to one value of  $V$ . Localization plane  $z = z_c$

of the considered vortex flows was taken in the near-surface layer  $z_c = 0.98$ , which corresponds to the drift velocity  $V = -0.4452$ .

#### 4.1 Non-central collision of two vortex monopoles

The nature of the collision of vortices depends on their polarity. First, let us consider the case when the vortices are oriented in the opposite way and have the same intensity in magnitude. For this case, the values of the parameters in the solution (11) and (13):  $N = 2$ ;  $C_1 = 1$  and  $C_2 = -1$ . The shift parameters  $b_j$  along the  $y$  coordinate are impact parameters. When they are equal to zero,  $b_1 = b_2 = 0$ , a central collision of vortices takes place. We will consider a non-central collision with parameters  $b_1 = 0$  and  $b_2 > 0$ , in the  $XY$ -plane, which is the localization plane  $z = z_c$  of the vortex flow (see (7)). We will denote the centers of the vortices by  $(x_{c1}, y_{c1})$  and  $(x_{c2}, y_{c2})$ , and the distance between them by  $\Delta x_c = |x_{c1} - x_{c2}|$  and  $\Delta y_c = |y_{c1} - y_{c2}|$ . Let us immediately note that, due to the long-range action of the localized solutions under consideration, the difference in the shift parameters along the  $x$  axis,  $a_1 - a_2$ , may differ from  $x_{c1} - x_{c2}$  even if the vortex monopoles are separated by a sufficiently large distance. By  $\psi_+$  and  $\psi_-$  we will denote the amplitudes of the anticyclonic and cyclonic vortices, respectively.

The flow fields  $\psi(x, y)$  in the localization plane  $z = 0.98$  during a non-central collision of vortex monopoles of different polarity and the same intensity are shown in Fig. 6. Areas of high pressure are indicated in red, areas of low pressure are indicated in blue. The cores of vortex monopoles are visible as compact thick colored spots: the red spot is an anticyclone, the blue spot is a cyclone.

It can be seen (Fig. 6) that when the vortex vortices approach each other, they begin to rotate around a single center until they take a vertical position at  $\Delta x_c = 0$ , forming a dipole (Fig. 6e). Figure 6f shows the locations of the vortex centers (cyclone and anticyclone) shown in Fig. 6a–e. The distance between vortices in a dipole  $\Delta y_c \approx 2.1$ . Comparing the colorbars in Fig. 6a and e we see that the intensity of the vortices in the dipole has dropped by approximately 20 percent relative to their original intensity. It should also be noted that the collision pattern (Fig. 6a–e) is symmetrical when the signs of  $a_1$  and  $a_2$  are

reversed. Figure 6f is also symmetrical about the line  $(x - Vt)_c = 0$ .

We are interested in how much the found distance between the vortices in the dipole and their amplitudes depend on the impact parameter  $b_2$ . Figure 7 shows the amplitudes  $\psi_+$  and  $\psi_-$  in the center ( $x_{c1} = x_{c2} = 0$ ) depending on the impact parameter  $b_2$  (another parameter  $b_1 = 0$ ). It can be seen that this dependence has a significantly non-monotonic character:  $\psi_+$  and  $\psi_-$  increase from zero and then oscillate around  $\pm 1$ . Moreover, their sum remains unchanged,  $\psi_+ + \psi_- = 0$ . From Fig. 7 it is clear that at  $b_2 = 0$  the distance between the centers of the vortices  $\Delta y_c = |y_{c1} - y_{c2}| = 0$ , but already at small  $b_2 > 0$   $\Delta y_c = 2.1$ , i.e. changes abruptly, and then up to the value of the parameter  $b_2 = 2$ , remains almost unchanged. The abrupt change in  $\Delta y_c$  at  $b_2 = 0 + (b_1 = 0)$  is quite unexpected, but has a simple explanation, which is given in Appendix 1. For parameter values  $b_2 > 2$  the distance between  $\psi_+$  and  $\psi_-$  begins to increase (Fig. 7). Thus, visualization of solution (11) allows us to estimate the distance between the centers of different-polar vortices when they form a dipole, which, at the parameter value  $K_r = 1.75$  is  $(\Delta y_c)_{\text{dip}} \approx 2.1$ .

It is of interest to consider the central collision of oppositely polar vortices, which corresponds to  $b_1 = 0$  and  $b_2 = 0$ , and, as before, we take  $C_1 = -C_2 = 1$ . In this case, with values of the shift parameters  $a_1 < 1.0$  and  $-a_2 < 1.0$ , the distance between centers of vortices  $\Delta x_c$  does not change and amounts to  $\Delta x_c \approx 2.1$ , i.e. a dipole is formed. As  $a_1$  and  $-a_2$  decrease, the intensity of the vortices in the dipole weakens. When  $a_1 = 0$  and  $-a_2 = 0$ , the intensity of each vortex becomes zero and the vortices disappear. Visualization of the central collision of oppositely polar vortices at  $a_1 \leq 1.0$  and  $-a_2 \leq 1.0$ , which explains the above, is presented in Appendix 2.

Visualization of the solution (11) and (13) for  $N = 2$ ,  $C_1 = C_2 = 1$ ,  $b_1 = 0$  and  $b_2 \leq 2$ , which corresponds to the collision of two unipolar vortices of the same intensity, occurs by merging the vortices (like two drops of liquid) with the formation of one general vortex. This can be observed in Fig. 8, built for the values of the impact parameters  $b_1 = 0$  and  $b_2 = 1$ .

In the case of a central collision of two unipolar vortices (parameters  $b_1 = b_2 = 0$ ), critical distance between the centers of vortices, less than which they



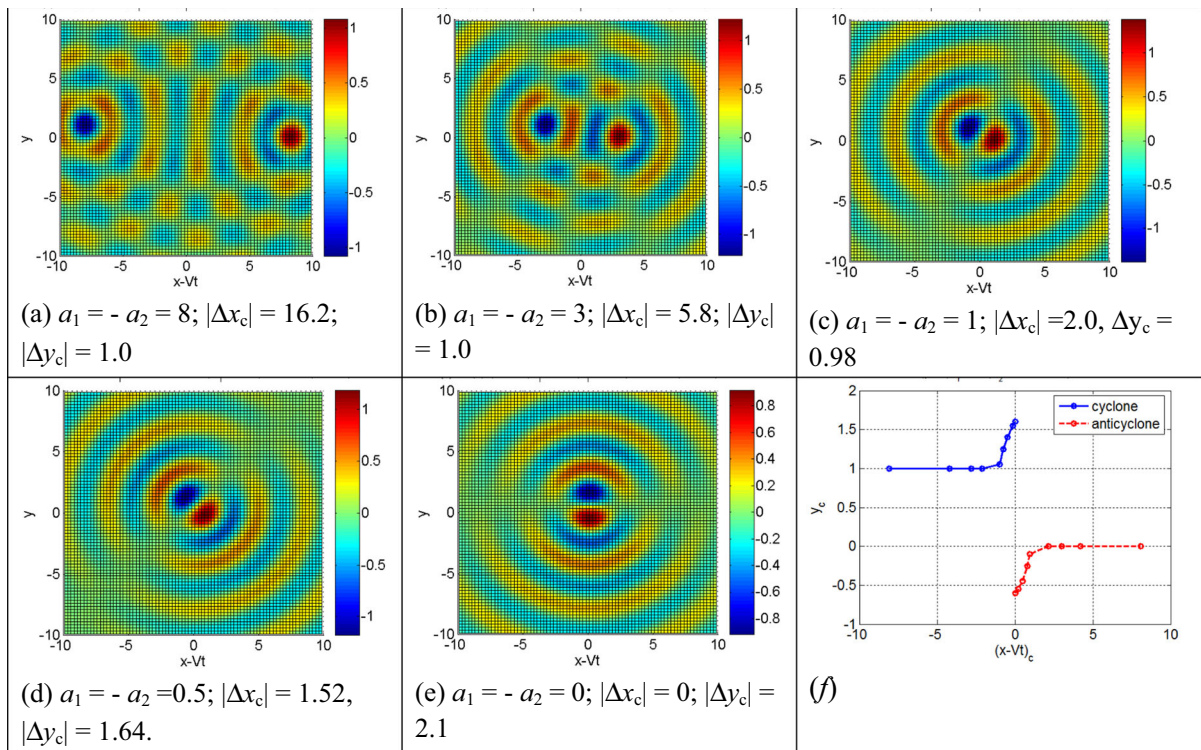


**Fig. 6 a–e** The flow field  $\psi(x, y)$  in the localization plane  $z = 0.98$  during an off-central collision of oppositely polarized vortices at  $C_1 = -C_2 = 1, b_1 = 0, b_2 = 1$ . Below each figure the shift parameters  $a_1$  and  $a_2$ , are shown for which they were

constructed, and the distances between the centers of the vortices along the  $x$  and  $y$  axes. **f** The locations of the vortex centers shown in Fig. 6 (a–e)

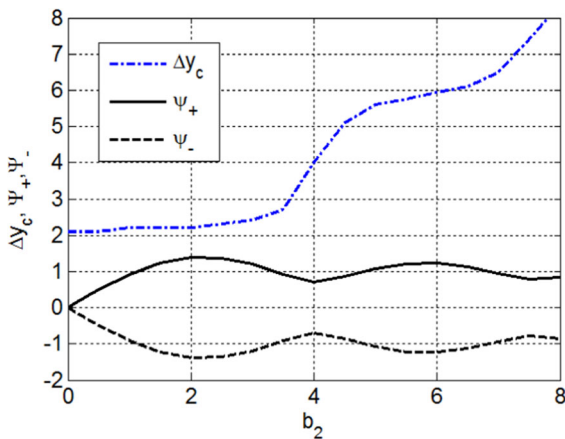


**Fig. 7** Vortex amplitudes ( $\psi_+$  and  $\psi_-$ ) at  $\Delta x_c = 0$  and the distance between the centers of the vortices  $\Delta y_c = y_{c1} - y_{c2}$  depending on the impact parameter  $b_2$ . Other parameters:  $b_1 = 0, a_1 = a_2 = 0, C_1 = -C_2 = 1, z_c = 0.98$

merge, for the case when the amplitudes of the vortices  $C_1 = C_2 = 1$  and  $K_r = 1.75$ , is  $(\Delta x_c)_{cr} = 1.803$ .

#### 4.2 An off-center “collision” of two oppositely oriented dipoles of equal intensity

The nature of the dipole collision depends on their orientation. If they are oriented in the same way, then, as the visualization of solution (11), (13) shows for  $N = 4$  and  $C_1 = -C_2 = C_3 = -C_4 = 1$ , their collision occurs according to the mechanism described at the end of Sect. 4.1. That is, the merging of dipoles occurs through the pairwise merging of vortices of the same polarity.

In this section we will briefly look at the off-center “collision” of two oppositely oriented dipoles. This task seems to us more interesting. In this case, the values of the parameters in (13):  $N = 4, -C_1 = C_2 = C_3 = -C_4 = 1$  and  $b_1 = -b_2 = 1.1, b_3 = 2.1, b_4 = -0.1$ . Here, by indices 1 and 2 we denote the parameters that relate to the right dipole, and by indices 3 and 4 – to the left dipole (see Fig. 9a). It was assumed that the shift parameters  $a_i$  ( $i = 1, 2, 3, 4$ )

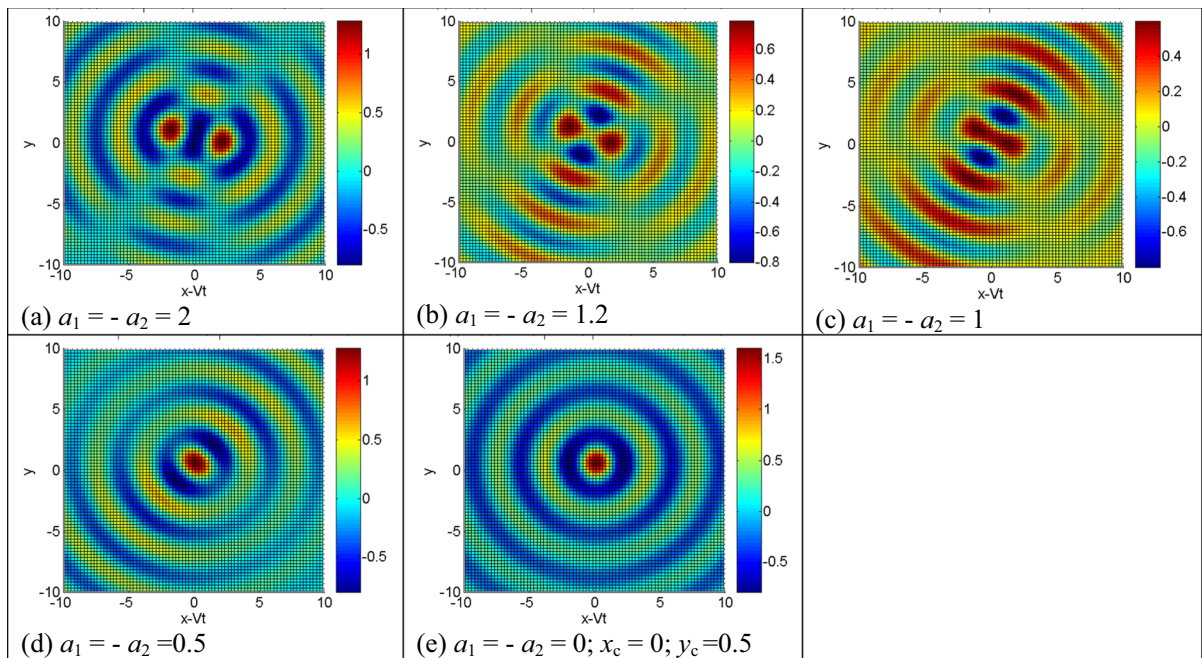


**Fig. 8 a–e** The flow field  $\psi(x, y)$  in the localization plane  $z = 0.98$  for an off-center collision of unipolar vortices at  $C_1 = C_2 = 1$ ,  $b_1 = 0, b_2 = 1$ . Below each figure the shift parameters  $a_1$  and  $a_2$  are shown for which they are constructed

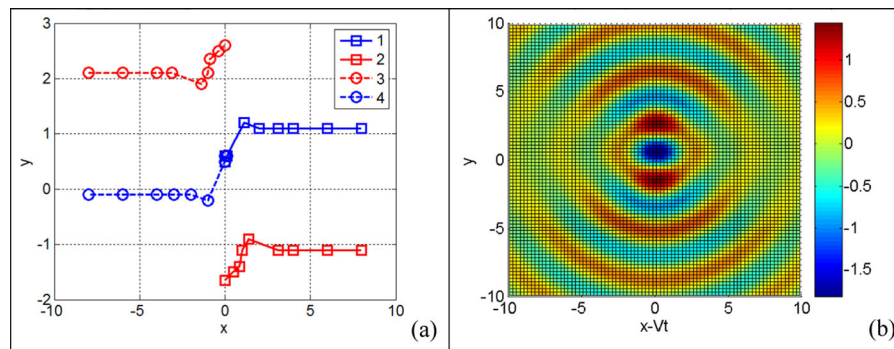


**Fig. 9** Off-center collision of two oppositely oriented dipoles of equal intensity,  $-C_1 = C_2 = C_3 = -C_4 = 1$ . Impact parameters  $b_1 = -b_2 = 1.1; b_3 = 2.1, b_4 = -0.1$ ; shift parameters

$a_1 = a_2 = -a_3 = -a_4 = a$ . **a** Locations of dipole vortex centers as parameter  $a$  decreases from 8 to 0. **b** Visualization of the geostrophic stream function  $\psi(x, y)$  at  $a = 0$

change in proportion to one parameter  $a$ :  $a_1 = a_2 = -a_3 = -a_4 = a$ .

$\approx 2.1$ , which is in good agreement with the result obtained in Sect. 4.1.

Figure 9a shows the locations of the dipole vortex centers as the parameter  $a$  decreases from 8 to 0. The picture in Fig. 9a is symmetrical when the signs of  $a_i$  are reversed. It can be seen that the cyclonic vortices in the dipoles merge at  $a = 0$ , forming a “tripole”, which is also shown in Fig. 9b by visualizing the geostrophic stream function  $\psi(x, y)$  at  $a = 0$ . The distance between the centers of neighboring vortices in a tripole is  $\Delta y_c$

It is important to note that the results of vortex interaction presented in Sect. 4 are qualitatively consistent with hydrodynamic modeling of oceanic vortices based on an  $N$ -layer shallow-water model [15].

### 5 Conclusion

The flow patterns of exact solutions of the (3 + 1)—dimensional nonlinear quasi-geostrophic equation of potential vorticity, also known as the Charney–Obukhov equation, for Rossby waves and vortices in the ocean propagating along the zonal direction with a constant velocity are considered. The exact solutions considered in this article were recently obtained by us in [12–14].

The main results of this work are as follows:

1)The vortices are localized in the vicinity of one or several planes  $z = z_{ci}, i = 1, 2, \dots, L$ , where  $0 \leq z_{ci} \leq H$  and  $L$  is the number of such planes, which depends on the drift velocity  $V$  and the values of the free parameters included in the  $U(z, V)$ , where  $U(z, V)$  is the velocity of the steady zonal background flow. The relationship between  $z_{ci}$  and  $V$  in the solutions is given by the Eq. (7)  $U(z_c; V) = 0, 0 \leq z_c \leq H$ . Examples of  $z_c(V)$  dependencies are shown in Fig. 1. Localization planes have a finite thickness, which can be estimated as  $\Delta z_c = O((C/H)^{1/2})$ , where  $C$  is the coefficient in the solution characterizing the intensity of the vortex and  $H$  is the ocean depth.

2)The model of a baroclinic dipole (heton) in the solution (11)–(13) for the ocean represents two vortices of different polarity, located in different planes of localization  $z = z_{ci}(V), (i = 1, 2)$ , one above the other, having a common center and common streamlines that propagate without changing the shape with the same constant velocity  $V$ , which is the drift

velocity of the dipole. There is a critical value of the velocity  $V_{cr}$  such that at  $V < V_{cr}$  there are no vortices, but as  $V$  increases, first one vortex  $z = z_c(V_{cr})$  appears, then at  $V > V_{cr}$  two localization planes appear  $z = z_{ci}(V)$ , in which two vortices are located. Vortexes in a dipole can have cylindrical symmetry (solution (11–13)) or spherical symmetry (solution (15)). A cylindrical—symmetrical heton can propagate both west and east at a velocity significantly exceeding the Rossby wave speed.

3)The “collision” of localized cylindrically symmetric Rossby vortices in the form of monopoles or dipoles located in the same plane of vortex localization  $z = z_c$  is described as a sequence of stationary solutions to the Charney-Obukhov equation. These solutions differ from each other in the values of the zonal coordinate shift parameters included in the solution. By changing the shift parameters, we can place the centers of the monopoles (or dipoles) at a given distance from each other, simulating both the process of their moving away from each other and their approach. The result of a non-central “collision” of vortex monopoles and dipoles depends on their polarity and their mutual orientation: two unipolar vortices merge, two oppositely polarized vortices form a dipole, two oppositely directed dipoles form a tripole upon “collision”. Note that the vortex collision results described above are in qualitative agreement with hydrodynamic modeling of oceanic vortices based on an  $N$ -layer shallow-water model [15].

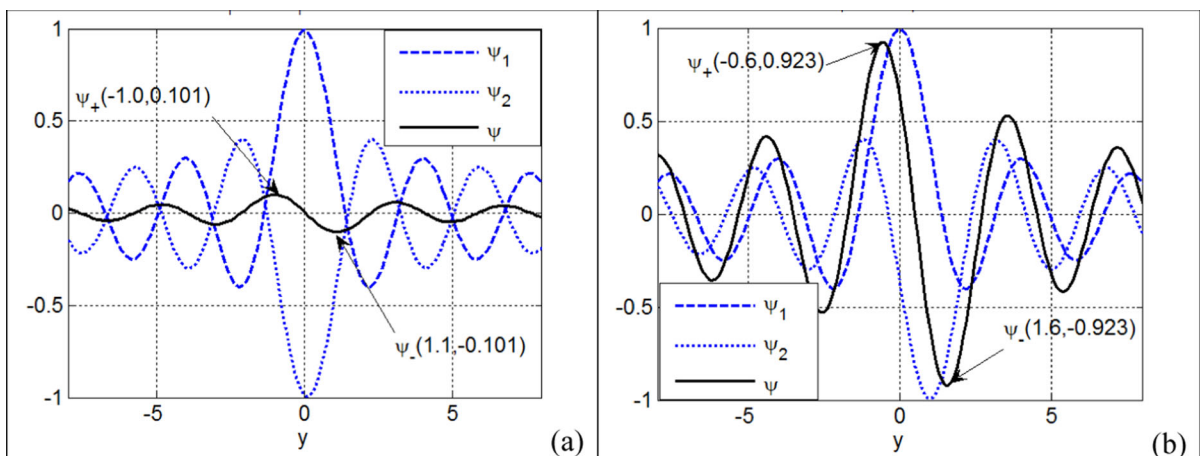
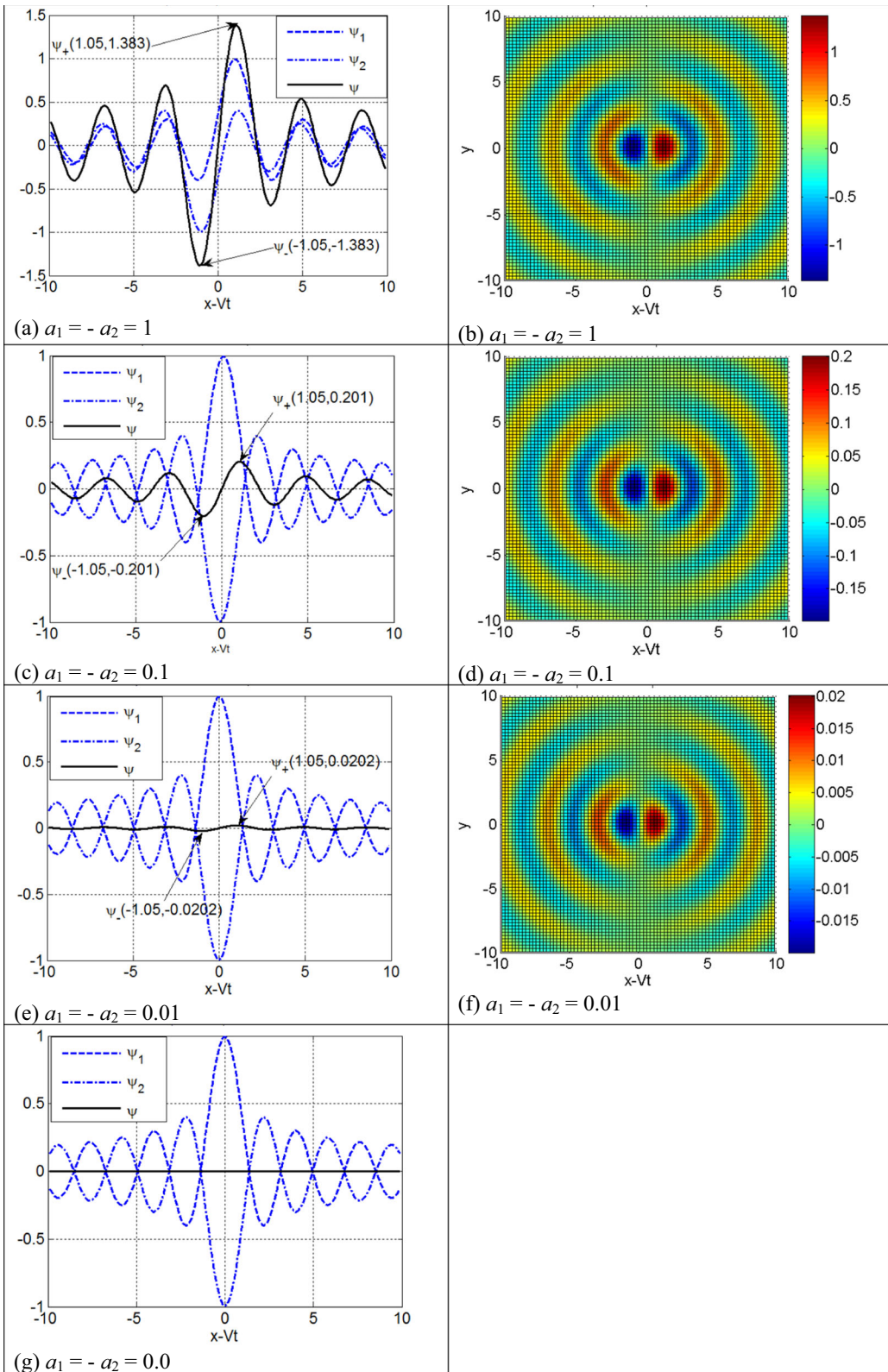


**Fig. 10** Example of estimating the amplitudes of monopoles  $\psi_+$  and  $\psi_-$  and the distance between them  $\Delta y_c$  in the section  $x-Vt = 0$  for impact parameters **a**  $b_1 = 0, b_2 = 0.1$ ; **b**  $b_1 = 0, b_2 = 1.0$ . Other parameters:  $a_1 = a_2 = 0, C_1 = -C_2 = 1, z = 0.98$







◀ **Fig. 11** Visualization of the central collision of oppositely polar vortices in solution (11), (13) for  $a_1 \leq 1.0$  and  $-a_2 \leq 1.0$ . The designations coincide with the designations in Fig. 10. The remaining parameters are  $b_1 = b_2 = 0$ ,  $C_1 = -C_2 = 1$ ,  $z = 0.98$ . Figures **b, d, f** show the stream function  $\psi(x, y)$ . Figures **a, c, e, g** are plotted in the section  $y = 0$  of the stream function  $\psi(x, y)$

**Author contributions** N.N. Myagkov: Conceptualization, Visualization, Writing- Original draft preparation. A.G. Kudryavtsev: Methodology, Software, Validation, Writing- Reviewing and Editing.

**Funding** The authors have not disclosed any funding.

**Data availability** No datasets were generated or analysed during the current study.

**Declarations**

**Conflict of interest** The authors declare no competing interests.

## Appendix 1

Figure 10 in the section  $x - Vt = 0$  shows the current function  $\psi$  of solution (11), (13) and functions  $\psi_1$  and  $\psi_2$  depending on  $y$ . Where  $\psi_1$  and  $\psi_2$  are defined as follows

$$\psi_j = \sin(k_z z_c) C_j J_0 \left( K_r \sqrt{(x - a_j - Vt)^2 + (y - b_j)^2} \right) + \left( -V + \frac{\beta(\sin(Kz)M + \cos(Kz) - 1)}{K^2} \right) y \quad (17)$$

where  $j = 1, 2$ . In the localization plane, due to (8) and (11), we have  $\psi = \psi_1 + \psi_2$ . Therefore, even with a small non-zero value of the parameter  $b_2$  (or  $b_1$ ) the dependence  $\psi(0, y)$ , as can be seen from Fig. 10, has a maximum ( $\psi_+$ ) and a minimum ( $\psi_-$ ) with the distance between them approximately equal to the width of the central hump of the Bessel function. It can be seen from the figure that when the parameter  $b_2$  changes by an order of magnitude, the distance between  $\psi_+$  and  $\psi_-$  practically does not change.

## Appendix 2

Visualization of the central collision of oppositely polar vortices in solution (11), (13) for  $a_1 \leq 1.0$  and  $-a_2 \leq 1.0$ . It can be seen (Fig. 11) that with a decrease in the shift parameters  $a_1$  and  $-a_2$ , the distance between the centers of the vortices  $\Delta x_c$  does not change and is  $\Delta x_c \approx 2.1$ , i.e. a dipole is formed. In this case, the intensity of the vortices in the dipole weakens. When  $a_1 = 0$  and  $-a_2 = 0$ , the intensity of each vortex becomes zero and the vortices disappear.

## References

- Pedlosky, J.: Geophysical Fluid Dynamics. Springer-Verlag, New York (1987)
- Petviashvili, V.I., Pokhotelov, O.A.: Solitary Waves in Plasmas and in the Atmosphere. Gordon Breach, London (1992)
- Connaughton, C., Nazarenko, S., Quinn, B.: Rossby and drift wave turbulence and zonal flows: the Charney-Hasegawa-Mima model and its extensions. Phys. Rep. **604**, 1–71 (2015). <https://doi.org/10.1016/j.physrep.2015.10.009>
- Bi, Y., Zhang, Z., Liu, Q., Liu, T.: Research on nonlinear waves of blood flow in arterial vessels. Commun. Nonlinear Sci. Numer. Simul. **102**, 105918 (2021). <https://doi.org/10.1016/j.cnsns.2021.105918>
- Umurhan, O.M.: Potential vorticity dynamics in the framework of disk shallow-water theory I. The Rossby wave instability. Astron. Astrophys. **521**, A25 (2010). <https://doi.org/10.1051/0004-6361/201015210>
- Ablowitz, M.J., Segur, H.: Solitons and the Inverse Scattering Transform. SIAM, Philadelphia (1981)
- Morozov, O.I.: A Lax Representation of the Charney-Obukhov Equation for the Ocean. Lobachevskii J. Math. **44**, 3973–3975 (2023). <https://doi.org/10.1134/S199508022309024X>
- Kaladze, T.D.: New solution for nonlinear pancake solitary Rossby vortices. Phys. Lett. A **270**, 93 (2000)
- Wang, J.Q., Zhang, R.G., Yang, L.G.: A Gardner evolution equation for topographic Rossby waves and its mechanical analysis. Appl. Math. Comput. **385**, 125426 (2020). <https://doi.org/10.1016/j.amc.2020.125426>
- Yin, X., Xu, L., Yang, L.: Evolution and interaction of soliton solutions of Rossby waves in geophysical fluid mechanics. Nonlinear Dyn. **111**, 12433–12445 (2023). <https://doi.org/10.1007/s11071-023-08424-8>
- Chen, L., Gao, F., Li, L., Yang, L.: A new three dimensional dissipative Boussinesq equation for Rossby waves and its multiple soliton solutions. Results Phys. **26**, 104389 (2021). <https://doi.org/10.1016/j.rinp.2021.104389>
- Kudryavtsev, A.G., Myagkov, N.N.: New exact spatially localized solutions of the (3 + 1) -dimensional Charney-Obukhov equation for the ocean. Phys. Fluids **34**, 126604 (2022). <https://doi.org/10.1063/5.0129694>

13. Kudryavtsev, A.G., Myagkov, N.N.: On exact solutions of the Charney Obukhov equation for the ocean. *Phys. Lett. A* **446**, 128282 (2022). <https://doi.org/10.1016/j.physleta.2022.128282>
14. Kudryavtsev, A.G., Myagkov, N.N.: On the superposition of solutions of the (3+1) dimensional Charney-Obukhov equation for the ocean. *Phys. Fluids* **35**, 051701 (2023). <https://doi.org/10.1063/5.0150230>
15. Carton, X.: Hydrodynamical modeling of oceanic vortices. *Surv. Geophys.* **22**, 179–263 (2001). <https://doi.org/10.1023/A:1013779219578>
16. Sokolovskiy, M.A., Verron, J.: Dynamics of vortex structures in a stratified rotating fluid. *Series Atmospheric and Oceanographic Sciences Library*, vol. 47. Springer, Cham (2014)
17. Reinaud, J.N., Carton, X.: The stability and the nonlinear evolution of quasi-geostrophic hetons. *J. Fluid Mech.* **636**, 109–135 (2009). <https://doi.org/10.1017/S0022112009007812>
18. Sokolovskiy, M.A., Koshel, K.V., Dritschel, D.G., Reinaud, J.N.: N-symmetric interaction of N hetons. I. Analysis of the case  $N = 2$ . *Phys. Fluids* **32**(9), 096601 (2020). <https://doi.org/10.1063/5.0019612>
19. Sutyryn, G.G., Radko, T., McWilliams, J.C.: Self-amplifying hetons in vertically sheared geostrophic turbulence. *Phys. Fluids* **33**(10), 101705 (2021). <https://doi.org/10.1063/5.0071017>
20. Kalashnik, M.V., Kurgansky, M.V., Chkhetiani, O.G.: Baroclinic instability in geophysical hydrodynamics. *Phys.-Usp.* **65**, 10 (2022). <https://doi.org/10.3367/UFNe.2021.08.039046>
21. Hughes, C.W., Miller, P.I.: Rapid water transport by long-lasting modon eddy pairs in the southern midlatitude oceans. *Geophys. Res. Lett.* **44**, 12375–12384 (2017). <https://doi.org/10.1002/2017GL075198>

**Publisher's Note** Springer Nature remains neutral with regard to jurisdictional claims in published maps and institutional affiliations.

Springer Nature or its licensor (e.g. a society or other partner) holds exclusive rights to this article under a publishing agreement with the author(s) or other rightsholder(s); author self-archiving of the accepted manuscript version of this article is solely governed by the terms of such publishing agreement and applicable law.